

Fig E1.

## Treatments

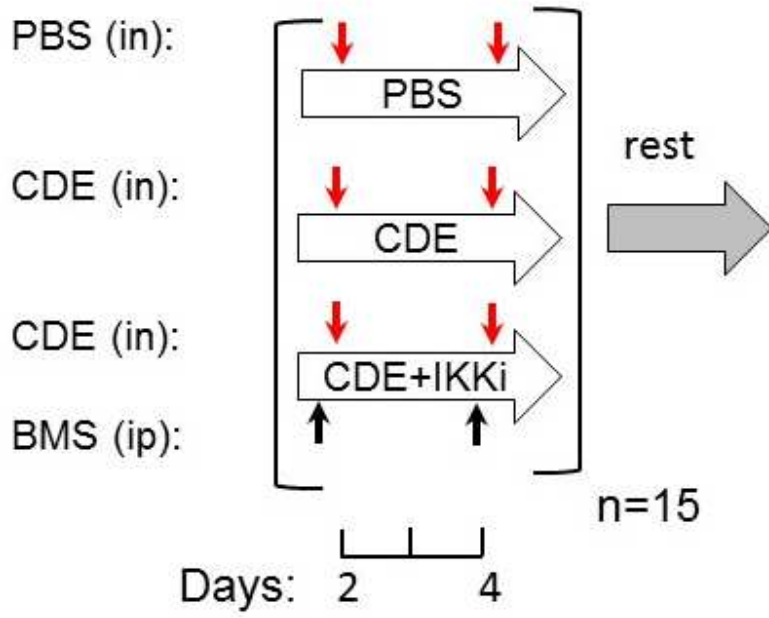


Fig E2

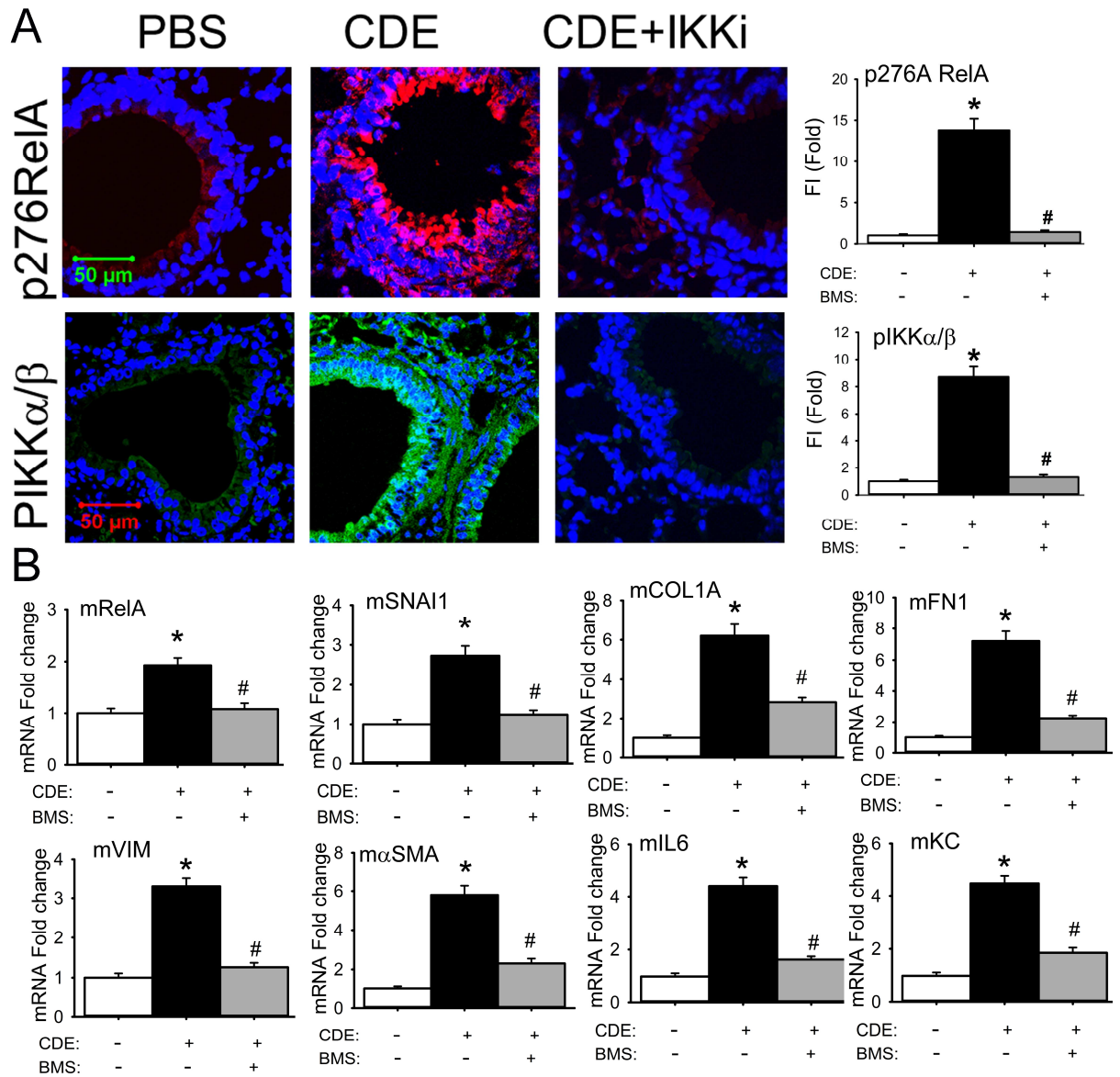


Fig E3

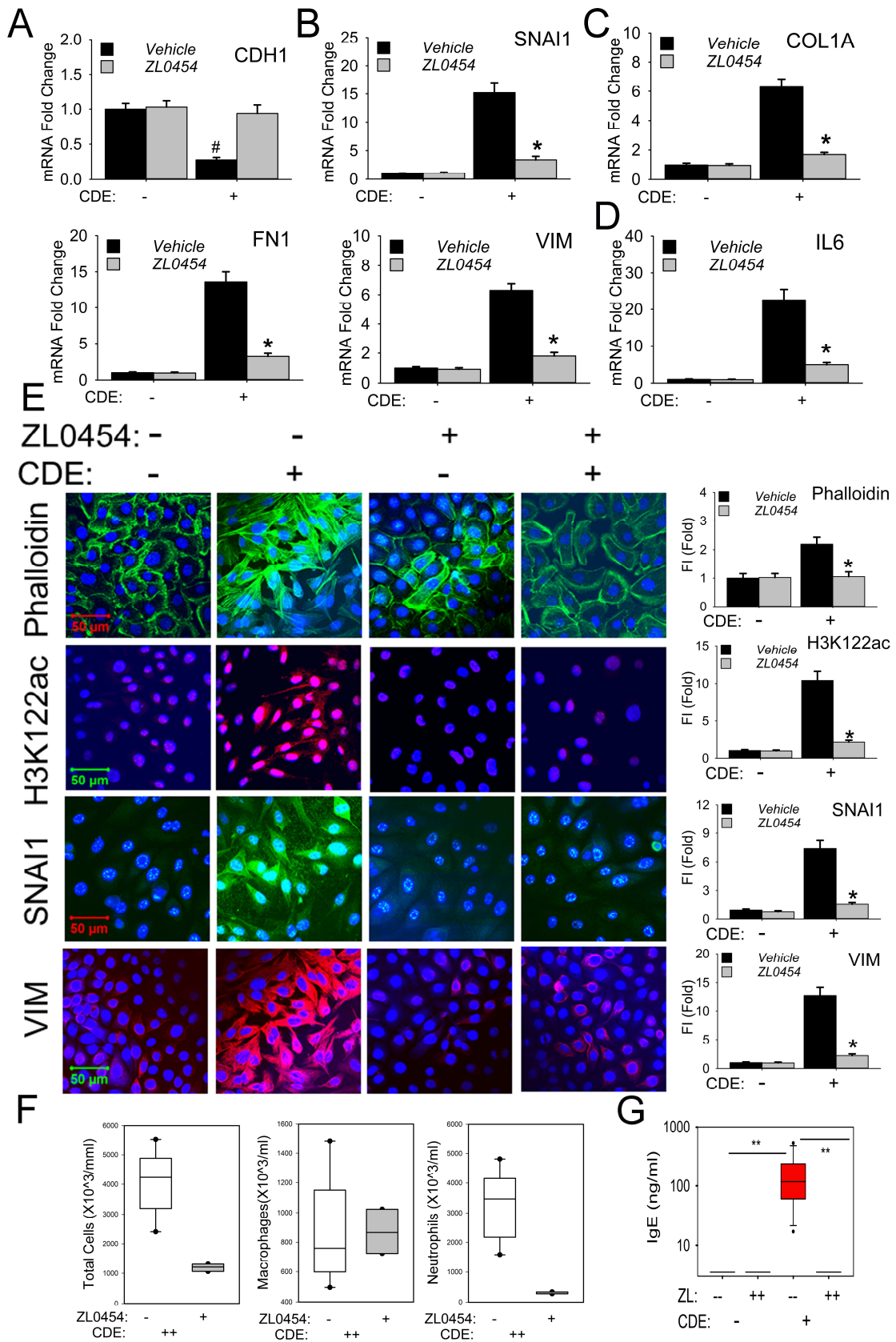


Fig E4

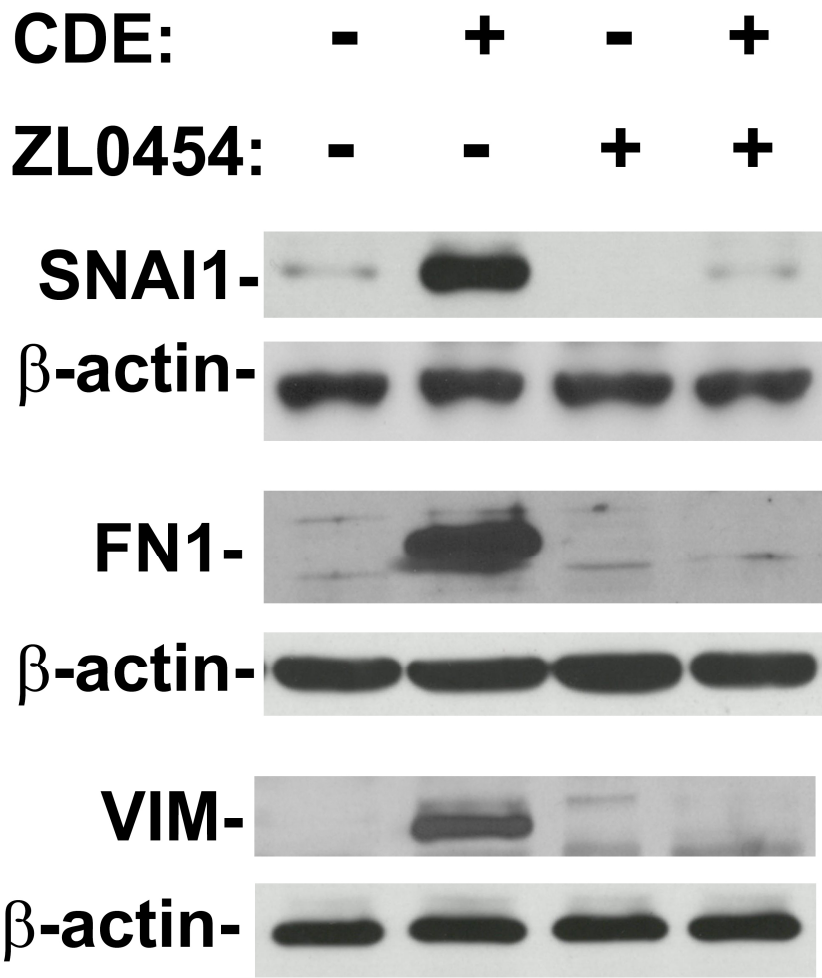


Fig E5

## 1 **Methods**

### 2 **Human subjects**

3 Human subjects were enrolled after providing informed consent to a protocol approved by the  
4 UTMB IRB. Demographic information was obtained to include duration of asthma, age at  
5 diagnosis, current medications, and history of exacerbations, in a manner consistent with our  
6 previous US SARP or US ACRN2 study protocols. Bronchial mucosal biopsies were obtained  
7 from the right middle and right lower lobes, and were stored in RNA Later®. Extracted total  
8 RNA from mucosal biopsy samples was analyzed for mRNA expressions of EMT genes using  
9 Q-RT-PCR.

10

### 11 **Cell culture and treatment**

12 Immortalized human small airway epithelial cells (hSAECs) were previously described  
13 (25). hSAECs were grown in SAGM small airway epithelial cell growth medium (Lonza,  
14 Walkersville, MD) in a humidified atmosphere of 5% CO<sub>2</sub>. BMS345541 was purchased from  
15 Sigma Aldrich. CDE was purchased from Greer Laboratories. The BRD4 selective small  
16 molecule inhibitor ZL0454 [(E)-4-((2-Amino-4-hydroxy-5-methylphenyl)diazenyl)-N-  
17 cyclopentylbenzenesulfonamide] was synthesized and characterized by instrumental analyses  
18 including NMR, mass spectrometry and, HPLC as described<sup>1</sup>. ZL0454 was used at 10 µM  
19 concentrations in cell culture medium and 10 mg/kg body weight *in vivo*.

20 hSAECs expressing a doxycycline (Dox)-regulated shRNA were produced by lentiviral  
21 transduction. TRIPZ Tet-on inducible lentiviral RelA shRNA and TRIPZ Inducible lentiviral empty  
22 vector shRNAs plasmids were commercially obtained (Dharmacon, GE Life Sciences, Lafayette,  
23 CO) and packaged after transfection of BOS23 cells. hSAECs were infected with collected  
24 virus-containing supernatants and selected for puromycin resistance (4 µg/ml). Puromycin  
25 resistant hSAECs were pooled and characterized. RelA depletion was produced by addition of  
26 doxycycline to the culture medium (2 µg/ml, 5 d).

27

## 28 **Animal studies**

29           Animal experiments were performed according to the NIH Guide for Care and Use of  
30 Experimental Animals and approved by the University of Texas Medical Branch (UTMB) Animal  
31 Care and Use Committee (approval no. 1312058A). Mice were housed under pathogen-free  
32 conditions with food and water ad libitum.

33

## 34 **Bronchoalveolar lavage and tissue processing**

35           Animals were anesthetized, bronchoalveolar lavage fluid (BALF) was obtained and the  
36 mice sacrificed. Lung tissues were taken for total RNA extraction or fixed for histological  
37 examination. For histological examination, lungs were inflated under 25 cm H<sub>2</sub>O pressure with  
38 10% (v/v) neutral buffered formalin through the tracheal cannula and immersed in 10 % buffered  
39 formalin for at least 24 h. After being processed into paraffin blocks, the lungs were cut into 5-  
40 µm sections and stained with Masson Trichrome to assess fibrotic changes. Microscopy was  
41 performed on a NIKON Eclipse Ti System <sup>2</sup>.

42           Periodic acid-Schiff (PAS) staining (pink color) was performed in parallel to demonstrate  
43 mucin secretion in airway epithelium <sup>3,4</sup>. Quantification of accumulated mucin was assessed by  
44 2 investigators who were blind to the treatment groups on a subjective scale of 0, 1, 2, 3, and 4  
45 corresponding to none, mild, moderate, marked, or severe mucin deposition, respectively. Data  
46 were expressed as means of scores recorded by 2 blinded investigators <sup>3,4</sup>.

47

## 48 **BALF analysis of cellular inflammation**

49           Cellular recruitment into the airway lumen was assessed in the collected  
50 bronchoalveolar lavage fluid (BALF) of mice. Lungs were perfused twice with 1 mL of sterile  
51 PBS (pH 7.4) and total cell counts determined by trypan blue staining and counting using a  
52 hemocytometer. Differential cell counts were performed on cytocentrifuge preparations

53 (Cytospin 3; Thermo Shandon, Pittsburgh, PA) stained with Wright-Giemsa. A total of 300 cells  
54 were counted per sample using light microscopy.

55

#### 56 **Quantitative Real-Time PCR (Q-RT-PCR)**

57 For gene expression analyses, 0.1 µg of cDNA product from reverse transcription of total  
58 RNA was amplified using SYBR Green Supermix (Bio-Rad) and gene-specific primers as  
59 previously described<sup>2,5</sup>. Quantification of relative changes in gene expression was calculated  
60 using the  $\Delta\Delta C_t$  method<sup>6,7</sup> and expression as the fold change between experimental and control  
61 samples was normalized to internal control peptidylprolyl isomerase A (PPI1A)/cyclophilin A.

62

#### 63 **Confocal Immunofluorescence Microscopy**

64 hSAECs were incubated ± CDE (20 µg/mL) for 15 d, re-plated on glass cover slips  
65 pretreated with rat tail collagen (Roche Applied Sciences), and fixed with 4% paraformaldehyde  
66 in PBS. Afterwards, the fixed cells were stained with Alexa Fluor® 488- or 568- phalloidin (Life  
67 Technologies) for cytoplasmic distribution of F-actin (green or red color) and also counterstained  
68 with 4', 6-diamidino-2-phenylindole (DAPI) for nuclear staining (blue color). The cells were  
69 visualized with a Nikon fluorescence confocal microscope at a magnification of 63X<sup>2,5</sup>.

70 For immunofluorescence staining, hSAECs were plated on rat tail collagen-treated cover  
71 glasses and stimulated with CDE for the indicated times. The cells were fixed with 4%  
72 paraformaldehyde in PBS and incubated with 0.1 M ammonium chloride for 10 min. Cells were  
73 permeabilized with 0.5% Triton-100, followed by incubation in blocking buffer (5% goat serum,  
74 0.1% IGEPAL CA-630, 0.05% NaN<sub>3</sub>, and 1% BSA) and incubated with primary antibodies of  
75 RelA (Santa Cruz. 1:300 dilution), VIM, SNAI1, CDH1, p267 RelA, H3K122ac, and pPol II Ser2  
76 (Abcam, 1:200 dilution) in incubation buffer (0.1% IGEPAL CA-630, 0.05% NaN<sub>3</sub>, and 2% BSA)  
77 overnight at 4 °C. After washing, cells were stained with Alexa Fluor 488- or 568--conjugated



78 goat anti-rabbit IgG (Life Technologies) respectively in incubation buffer for 1 h, then visualized  
79 with a LSM510 fluorescence confocal microscope, magnification 63X<sup>2,5</sup>.

80 Confocal Immunofluorescence assays of lung sections were performed on formalin-  
81 fixed, paraffin-embedded sections after rehydration using serial concentrations of ethanol.  
82 Antigen retrieval was performed in Tris-EDTA buffer (pH 9.0). Lung sections were blocked  
83 using 0.1% Triton-X, 5% normal goat serum in phosphate buffered saline (PBS) and incubated  
84 with primary antibodies of rabbit anti-p276RelA, pIKK $\alpha/\beta$ , SNAI1, H3K122ac, COL1A, VIM, FN1,  
85 and  $\alpha$ SMA (Abcam, 1:200 dilution) overnight at 4°C. Normal anti-rabbit IgG were used as  
86 staining specificity controls. After washing, lung sections were stained with Alexa Fluor 488- or  
87 568- conjugated goat anti-rabbit IgG (Life Technologies) in incubation buffer for 1 h. Nuclei  
88 were stained with 4', 6-diamidino-2-phenylindole (DAPI) (5  $\mu$ g/ml in PBS, 20 min) and mounted  
89 slides visualized with a LSM510 fluorescence confocal microscope, magnification 63X.

90

### 91 **IgE measurement**

92 Total IgE in serum were measured using Sandwich ELISA. 96-well plates 4 HBX  
93 (Thermo Scientific, Hudson, NH, USA) were coated with the purified rat anti-mouse IgE capture  
94 antibody (BD Biosciences, San Jose, CA, USA) for 2 hours at room temperature. After three  
95 washing, the plates were blocked with Sea Block blocking buffer (Pierce Biotechnology, Inc,  
96 Rockford, IL, USA). Serum were added and incubated overnight. After washing, the plates were  
97 incubated with biotin-conjugated rat IgE (BD Biosciences, San Jose, CA, USA) for 2 hours at  
98 room temperature, then washed and incubated with avidin-conjugated alkaline phosphatase for  
99 45 minutes at 4°C. After washing, fluorometric values for each well were measured after  
100 addition of AttoPhos substrate solution (Promega, Madison, WI, USA)<sup>3,4</sup>.

101 Cat dander-specific IgE measurement was performed on 96-well plates. Plates were  
102 coated with 100  $\mu$ g/ml of cat dander protein overnight at room temperature and blocked for 2  
103 hour with sea block buffer. Plates were applied with serum overnight. After washing, the plates

104 were incubated with biotin-conjugated rat IgE (BD Biosciences, San Jose, CA, USA) for another  
105 2 hours at room temperature, then washed and incubated with avidin-conjugated alkaline  
106 phosphatase for 45 minutes at 4°C. After washing, fluorometric values for each well were  
107 measured after addition of AttoPhos substrate.

108

### 109 **Analysis of collagen content**

110 To estimate amount of collagen in the lung tissue and BALF, hydroxyproline content was  
111 measured colorimetrically using a hydroxyproline assay kit (Sigma-Aldrich, St. Louis, MO) with  
112 minor modifications (24, 25). Briefly, the lungs were weighed, homogenized in liquid nitrogen  
113 with 2 ml PBS, after which 2.0 ml of 12 N HCl was added, and the samples were hydrolyzed at  
114 120 °C within a PTFE-lined capped pressure-tight vial for 6 h. Separately, 100 µl of BALF was  
115 hydrolyzed with 12 N HCl as above. Afterwards, 10 µl hydrolyzed samples were mixed with 100  
116 µl of chloramine T/oxidation buffer at room temperature for 5 min and later incubated with the 4-  
117 (Dimethylamino) benzaldehyde (DMAB) reagent for 90 min at 60 °C. The absorbance of  
118 oxidized hydroxyproline was determined by absorbance 560 nm (Infinite M200 PRO multimode  
119 microplate reader, Tecan Instruments). Standard curves were generated for each assay using  
120 hydroxyproline standards. The amount of collagen was expressed in micrograms per milligram  
121 lung tissue while it was expressed in nanograms per milliliters in BALF. The data shown are the  
122 means ± S.D. from n=5 experiments.

123

### 124 **Stable isotope dilution (SID)-selected Reaction Monitoring (SRM)-mass spectrometry** 125 **(MS)**

126 The selection of the signature peptides for targeted MS-based quantification of BRD4, Pol II,  
127 H3, and H4 used a published workflow<sup>8</sup>. Stable isotope-labeled signature (SIS) peptide  
128 standards were chemically synthesized incorporating isotopically labeled [13C615N4] Arginine  
129 or [13C615N2] Lysine to a 99% isotopic enrichment (Thermo Scientific). BALF proteins were

130 digested with trypsin. Afterwards, an aliquot of 5  $\mu$ L of stable isotope-labeled signature peptides  
131 was added to each tryptic digest. These samples were desalted with a ZipTip C18 cartridge  
132 before MS analysis. The SRM transitions for the signature peptides and their stable isotope  
133 label standard peptides are tabulated in **Table E2**. All data are shown as the ratio of target to  
134 SIS peptide and represent a mean  $\pm$  S.D. from n=5 animals with technical replicates.

135

### 136 ***In Situ* Proximity Ligation Assay (PLA)**

137 Paraffin embedded lung section slides were subjected to antigen retrieval, permeabilized  
138 with 0.1% Triton X-100, and incubated with IgG or primary rabbit Ab to RelA (Santa Cruz), and  
139 mouse Ab to BRD4 (Sigma Aldrich). Slides were then subjected to PLA using the Duo-link PLA  
140 kit from O-Link Bioscience (Uppsala, Sweden) according to the manufacturer's instructions. The  
141 nuclei were counterstained with DAPI, and the PLA signals were visualized in a LSM510  
142 fluorescence confocal microscope at 63X Magnification.

143

### 144 **References**

- 145 1. Tian B, Liu Z, Yang J, Sun H, Zhao Y, Wakamiya M, et al. Selective Molecular  
146 Antagonists of the Bronchiolar Epithelial NF $\kappa$ B-Bromodomain-Containing Protein 4  
147 (BRD4) Pathway in Viral-induced Airway Inflammation. *Cell Reports* 2018; 23:1138-51.
- 148 2. Tian B, Patrikeev I, Ochoa L, Vargas G, Belanger KK, Litvinov J, et al. NF $\kappa$ B  
149 Mediates Mesenchymal Transition, Remodeling and Pulmonary Fibrosis in Response to  
150 Chronic Inflammation by Viral RNA Patterns. *Am J Respir Cell Mol Biol* 2016.
- 151 3. Hosoki K, Aguilera-Aguirre L, Brasier AR, Kurosky A, Boldogh I, Sur S. Facilitation of  
152 Allergic Sensitization and Allergic Airway Inflammation by Pollen-Induced Innate  
153 Neutrophil Recruitment. *Am J Respir Cell Mol Biol* 2016; 54:81-90.
- 154 4. Hosoki K, Boldogh I, Aguilera-Aguirre L, Sun Q, Itazawa T, Hazra T, et al. Myeloid  
155 differentiation protein 2 facilitates pollen- and cat dander-induced innate and allergic  
156 airway inflammation. *J Allergy Clin Immunol* 2016; 137:1506-13.e2.
- 157 5. Tian B, Zhao Y, Sun H, Zhang Y, Yang J, Brasier AR. BRD4 Mediates NF $\kappa$ B-dependent  
158 Epithelial-Mesenchymal Transition and Pulmonary Fibrosis via Transcriptional  
159 Elongation. *The American Journal of Physiology -Lung Cellular and Molecular*  
160 *Physiology* 2016; 311:L1183-L201.
- 161 6. Tian B, Li X, Kalita M, Widen SG, Yang J, Bhavnani SK, et al. Analysis of the TGF $\beta$ -  
162 induced program in primary airway epithelial cells shows essential role of NF-  
163 kappaB/RelA signaling network in type II epithelial mesenchymal transition. *BMC*  
164 *Genomics* 2015; 16:529.

- 165 7. Tian B, Zhao Y, Kalita M, Edeh CB, Paessler S, Casola A, et al. CDK9-dependent  
166 transcriptional elongation in the innate interferon-stimulated gene response to respiratory  
167 syncytial virus infection in airway epithelial cells. *J Virol* 2013; 87:7075-92.
- 168 8. Zhao Y, Brasier AR. Applications Of Selected Reaction Monitoring (SRM)-Mass  
169 Spectrometry (MS) For Quantitative Measurement Of Signaling Pathways. *Methods*  
170 2013; 61:313-21.

171

172

173 **Table E1. Clinical demographics of human subjects.** MMA, mild-moderate  
 174 asthma; FEV1, forced expiratory volume in 1 sec; FVC, forced vital capacity; %, percent  
 175 predicted. ICS, inhaled corticosteroid, LABA, long-acting  $\beta$ 2 agonist, SABA, short-acting  $\beta$ 2  
 176 agonist.

	<b>AGE:</b>	<b>SEX</b>	<b>Treatment:</b>	<b>STATUS</b>	<b>FEV1</b>	<b>FVC</b>
<b>1.</b>	33	M	None	Normal	4.72	5.70
<b>2.</b>	28	F	None	Normal	3.37	3.75
<b>3.</b>	30	M	None	Normal	3.67	4.61
<b>4.</b>	31	M	None	Normal	4.07	4.95
<b>5.</b>	26	F	None	Normal	3.67	4.20
				average	3.9	4.642
<b>6.</b>	56	F	ICS, SABA	Mild Moderate	2.52	3.05
<b>7.</b>	28	M	ICS, SABA	Mild Moderate	2.71	4.30
<b>8.</b>	55	F	ICS, SABA	Mild Moderate	2.07	2.76
<b>9.</b>	29	M	SABA , LABA, ICS	Mild Moderate	4.31	6.95
<b>10.</b>	56	F	ICS, SABA	Mild Moderate	2.16	2.87
<b>11.</b>	46	F	LABA	Severe	2.53	3.02
<b>12.</b>	51	F	ICS, SABA	Severe	0.78	1.74
				average	2.44	3.53

**Table E2. SID-SRM-MS parameters for airway remodeling protein**

Protein Name	Uniprot #	Gene Name	Sequence	Q1, m/z	Q3, m/z	Precursor ion Z	Product ion Z	ion type	CE (V)
<b>Fibronectin</b>	P11276	Fn1	VFAVHQGR	457.2537	596.3257	2	1	y5	18.8606
			VFAVHQGR	457.2537	667.3629	2	1	y6	18.8606
			VFAVHQGR	457.2537	814.4313	2	1	y7	18.8606
			VFAVHQGR	457.2537	913.4997	2	1	y8	18.8606
			VFAVHQGR[13C615N4]	462.2579	606.334	2	1	y5	19.0308
			VFAVHQGR[13C615N4]	462.2579	677.3712	2	1	y6	19.0308
			VFAVHQGR[13C615N4]	462.2579	824.4396	2	1	y7	19.0308
			VFAVHQGR[13C615N4]	462.2579	923.508	2	1	y8	19.0308
<b>SPARC-like protein 1</b>	Q14515	Sparcl1	ILTHSELAPLR	625.3667	698.419	2	1	y6	24.5765
			ILTHSELAPLR	625.3667	785.451	2	1	y7	24.5765
			ILTHSELAPLR	625.3667	922.5099	2	1	y8	24.5765
			ILTHSELAPLR[13C615N4]	630.3709	708.4272	2	1	y6	24.7466
			ILTHSELAPLR[13C615N4]	630.3709	795.4593	2	1	y7	24.7466
			ILTHSELAPLR[13C615N4]	630.3709	932.5182	2	1	y8	24.7466

**Fig E1. Chronic CDE stimulation induces mesenchymal transition of airway epithelial cells.** **A**, Confocal immunofluorescence micrographs of human small airway epithelial cells (hSAECs) incubated in the absence or presence of CDE (20 µg/mL) for 15 days. Cells were stained with Alexa568-conjugated phalloidin (red color) and DAPI (a nuclear DNA stain, blue color). Graphs are shown at 63X magnification. **B**, Q-RT-PCR assays of total RNA extracted from a time course of CDE-stimulated hSAECs for the epithelial marker *CDH1* (E-cadherin). Shown as fold-change mRNA abundance normalized to *PPIA* (*cyclophilin A*). \*  $p < 0.01$ ,  $n = 3$ . **C**, Q-RT-PCR of *SNAI1* and *RelA* mRNAs. **D**, Q-RT-PCR for vimentin (*VIM*), collagen 1A (*COL1A*), fibronectin (*FN1*), and *MMP9*. **E**, Q-RT-PCR for expression of paracrine growth factor *IL6* and *TGFβ* mRNA. **F**, Q-RT-PCR for *CXCL8/IL8*. **G**, Q-RT-PCR for inducible NADPH oxidase, *NOX4*. All Q-RT-PCR data are the means ± S.D. from  $n = 3$  experiments. \*,  $p < 0.05$ , compared to without CDE, t-test.

**Fig E2. Repetitive CDE (rCDE) exposure *in vivo*.** Schematic of experimental strategy. 18 week-old C57BL/6 mice were pretreated IKK inhibitor BMS345541 (10 mg/kg body wt, ip;  $n = 5$ ) or vehicle and were subjected to  $n = 15$  challenges with intranasal (in) CDE (20 µg/dose) every other day for a total of 30 d. Shown is the timing of the administration for each of the treatment groups. Red vertical arrows, administration of PBS or CDE via the in route; black arrows, administration of CDE via the ip route. 12 days after the last CDE challenge, mice were sacrificed and analyzed.

**Fig E3. rCDE exposure activates NFκB pathway and mesenchymal program in the airway mucosa.** **A**, Confocal immunofluorescence micrographs of phospho-Ser 276 RelA (p276RelA, red) or phospho-IKK α/β (green), counterstained with DAPI in representative lung sections from PBS, CDE or BMS+CDE treated mice. Images were acquired at 63X magnification. At right are quantifications of relative fluorescence intensity in 5 independent images. \*,  $p < 0.05$ , compared to without CDE; #,  $p < 0.05$  compared to CDE alone. **B**, Q-RT-PCR of total RNA from lung tissues of PBS, CDE or BMS+CDE treated mice. Shown is fold change in mouse (m) mRNA expression for each gene normalized to *PPIA*. \*,  $p < 0.01$ , compared to without CDE; #,  $p < 0.01$  compared to CDE alone,  $n = 5$ , t-test.

**Fig E4. BRD4 pathway mediates CDE-induced EMT of airway epithelial cells.** WT hSAECs were treated with CDE (20 µg/mL) for 0 or 15 d in the presence or absence of BRD4 inhibitor ZL0454 (10 µM) before harvesting for Q-RT-PCR and performing confocal immunofluorescence microscopy. **A**, Q-RT-PCR for *CDH1* mRNA expression. #,  $p < 0.01$ , compared to without CDE,  $n = 3$ , T-test. **B**, Q-RT-PCR for *SNAI1* mRNA expression. \*,  $p < 0.01$ , compared to CDE alone,  $n = 3$ . **C**, Q-RT-PCR for *COL1A*, *FN1*, and *VIM* mRNA expression. **D**, Q-RT-PCR for *IL6* mRNA expression. **E**, Confocal immunofluorescence microscopy for phalloidin (green color), H3K122-Ac (red color), *SNAI1* (green color), and *VIM* (red color) counterstained with DAPI (blue color) in WT hSAECs in absence or presence of CDE (20 µg/mL, 15d) stimulation. Images were acquired at 63X. At right are quantifications of relative fluorescence intensities of phalloidin, H3K122ac, *SNAI1*, and *VIM*, \*  $p < 0.01$ ,  $n = 5$ , t-test. **F**, Mice were treated in absence or presence of ZL0454 (10 mg/kg) prior to acute intranasal challenge of CDE. Shown are total, macrophage, and neutrophil counts in BALF 24 h later after CDE challenge. **G**. Total serum IgE was quantitated for each chronic treatment group, \*\*,  $p < 0.01$ ,  $n = 5$ , t-test.

**Fig E5. BRD4 inhibitor blocks rCDE-induced SNAI1, FN1, and VIM accumulation in lung tissue.** 300 µg homogenized whole lung extracts of mice were fractionated by SDS-PAGE and subjected to western immunoblot with SNAI1, FN1, and VIM Abs, β-actin was probed as loading controls. Similar results were found in experiments repeated three times independently.